CHAPTER 66

DISSIPATION OF DEEP WATER WAVES BY HYDRAULIC BREAKWATERS

by

R. E. Nece,[1] E. P. Richey,[2] and V. Seetharama Rao[3]

ABSTRACT

Experimental results are presented for a laboratory study of the effectiveness of hydraulic breakwaters in dissipating deep water waves. Test data are reported for a range of wave steepnesses for wave length: water depth ratios ranging from 0.375 to 1.343.

It is shown that the effectiveness of hydraulic breakwaters depends upon the steepness of the incident wave and upon the ratio of the momentum of the opposing surface current created by the breakwater to the momentum of the incident waves. Results also are compared with the theoretical predictions of Taylor which are appropriate to deep water waves.

Data are presented in a form allowing the determination of hydraulic breakwater manifold discharge characteristics in order to achieve specified attenuation for a particular incident wave. It is concluded that while the hydraulic breakwater is better adapted to deep water waves than to shallow water waves upon which prior studies of the device have concentrated, it is generally inefficient for most practical cases because of excess power requirements. Some possible field applications are indicated.

INTRODUCTION

The hydraulic breakwater is a device which uses a series of horizontal water jets to generate a surface current opposed to the direction of propogation of incident waves; the surface current produces attenuation and/or breaking of the waves. Hydraulic breakwaters have been studied rather extensively by means of laboratory experiments. Quite logically, experimental data have emphasized the behavior of these devices in intermediate-depth water waves ($2 < L/d < 20$), because it has been considered that this type of wave attenuating device would be most useful in installations near the coast. Representative laboratory studies of hydraulic breakwaters have been reported by Evans (1955), Straub et al (1958), and Williams (1960); while some data for deep water waves ($L/d < 2$) are included, these are very limited. The above listing is not a complete

1. Professor of Civil Engineering, University of Washington, Seattle, Washington.
2. Associate Professor of Civil Engineering, University of Washington, Seattle, Washington.
3. Hydraulic Engineer, Lewis-Redford-Engineers, Bellevue, Washington.

one, and is restricted to two-dimensional wave tank studies. Williams and Wiegel (1963) examined the effect of a surface located hydraulic breakwater on wind generated waves, and found that shorter, steeper wave components were attenuated to a greater degree than were the longer wave components.

Growing interest in such structures as floating bridges and pontoon-type marinas which might be located close to shore but which are still in a deep water environment so far as surface waves are concerned has prompted further consideration of the possibility of using hydraulic breakwaters for attenuation of deep water waves. The structures mentioned commonly have plane vertical sidewalls of finite depth which can cause reflection of the incident waves. A suggested application of the hydraulic breakwater is to attach it outboard of such structures in order to attenuate the incident waves before they reach the structure and hence minimize wave reflections which may be undesirable. Currents created by the hydraulic breakwater are confined to a thin zone near the water surface, and for deep water waves the wave energy likewise is concentrated near the surface. It has been agreed generally that hydraulic breakwaters should be expected to provide their best performance in deep water; for shallow water waves, the device has been found relatively inefficient.

The actual physical mechanism by which the breakwater's opposing surface current modifies a wave still is not fully understood. If the incident wave is originally steep and if the current is strong, varying degrees of wave breaking may occur. On the other hand, waves may be damped without breaking taking place. Guidance for the predicted effectiveness of hydraulic breakwaters in deep water is given in the theoretical solution of Taylor (1955). The solution, which is based upon linear wave theory and therefore does not consider the effect of wave height, predicts the longest wave length that may be propogated against a surface current having a finite thickness and a velocity varying linearly from a maximum at the surface to zero at the bottom edge of the current.

Because Taylor's theory considers only the complete stopping of waves and therefore does not consider less than complete wave attenuation, and because previous experimental data were very limited for deep water waves, an experimental program was conducted to study the effectiveness of hydraulic breakwaters in deep water waves.

EXPERIMENTAL APPARATUS AND PROCEDURE

Wave Tank - A schematic drawing of the wave tank used is shown in Figure 1. Pertinent dimensions were: length (excluding forebay), 35 ft. 5 in.; width, 24 inches; depth, 35 inches. The effective length of tank measured from wave generator to absorber beach was 27 ft. 3 in. The tank was a laboratory flume which was converted to a wave tank for the breakwater study. Because the tank was relatively short for wave studies it was equipped with an absorber beach consisting of aluminum turnings loosely packed in wire mesh baskets, with the baskets on the sloping portion of the beach located on an impervious plane support. This type of arrangement has been discussed by Hsu (1965). The reflection coefficient of the beach was approximately 5 percent.

Generator - The flap type generator, made from 1/2-inch aluminum plate, was hinged to the bottom of the wave channel. Both the frequency and the stroke amplitude could be changed in discrete steps. For the experiments presented in this paper the water depth was maintained constant at 32 in. (2.67 ft.), and waves of only four periods were tested, each with a number of discrete wave heights (therefore, steepnesses). The properties of the waves tested are given in the following table; the measurements were made with the manifold removed from the tank.

Period, T (Sec.)	Length, L (ft.)	L/d	Height, H (ft.)	Steepness H/L
0.45	1.00	0.375	0.046	0.046
			.074	.074
			.095	.095
0.53	1.42	0.532	0.049	0.035
			.078	.055
			.100	.071
			.152	.107
0.67	2.33	0.875	0.050	0.021
			.077	.033
			.102	.044
			.146	.063
			.180	.077
0.84	3.58	1.343	0.044	0.012
			.072	.020
			.094	.026
			.139	.039
			.178	.050

Breakwater - The cylindrical manifold completely spanned the wave tank. The manifold was constructed of 1-1/4 in. O.D. plastic tubing with a 1/8-in. wall thickness, and contained 93 circular orifices of 0.04-in. diameter at 1/4-in. spacing. The breakwater discharge was supplied to the manifold by a single inlet pipe at mid-channel. The large number of discharge ports was selected in order to develop a two-dimensional current as close as possible to the manifold. For all runs reported the submergence depth y_o (Figure 2) of the manifold centerline was 0.1-ft., sufficient to have the jets discharging submerged for all waves tested; jet discharge was horizontal.

Discrete flow rates q, in terms of cfs/ft of tank width, were: 0, 0.002, 0.004, 0.005, 0.006, 0.00725. Discharges were measured with a calibrated orifice located in the recirculating loop.

Wave Height Measurements - Wave heights were measured by resistance-type wire gages, the outputs being obtained on a recording oscillograph. Accuracy of measured wave heights was $\pm$ 0.002-ft.

Because of the relative shortness of the wave tank the following procedures were adopted for wave height measurements. All waves were

measured at the gage location shown in Figure 1. As indicated above, values of the incident wave height (Figure 2) were determined with the manifold removed from the channel. For the case of the manifold in place but not discharging ($q = 0$), as with the determination of H, the heights of a number of waves were averaged soon after regular waves were sensed at the gage. For the transmitted waves H_t with the manifold discharging, the finite size of the tank necessitated the following procedure. The breakwater discharge was started, and then the wave generator. The average of the first three or four waves was taken immediately after recorded wave heights at the gage had reached their maximum and when the heights of successive waves were approximately the same. Tests were repeated to check for reproducibility, but all data points are presented as separate values and not as averages of a number of runs. As noted by previous investigators, the value of H_t never reached a constant value; part of this could be due to randomness associated with the interaction between incident waves and turbulent surface currents, and part to recirculation patterns resulting in the finite-sized tank. Further, for the longest wave tested the gage was less than two wave lengths behind the generator, which could put it in the area in which the waves reforming after passing the manifold still might be regaining amplitude.

Measurement of Breakwater Current Velocities - Currents were measured in the absence of waves. A 1/8-in. O.D. Prandtl tube mounted so as move longitudinally and vertically was used as the sensor. Data reported were taken on the channel centerline, but separate checks indicated the flow patterns to be satisfactorily two-dimensional. The Prandtl tube was used in conjunction with a differential pressure transducer and an X-Y plotter for recording data; the static calibration corresponded to a range of velocities from 5 to 28 in. per second. Velocity values reported were time-averaged values existing approximately 1 - 1-1/2 minutes after the breakwater current had been started in initially still water; this time coincided with that during which the values of H_t were measured in the attenuation runs.

EXPERIMENTAL RESULTS AND ANALYSIS

Breakwater Currents - Some results of the velocity measurements in the surface currents created by the breakwater manifold are given in Figures 3 - 6. These results are discussed briefly.

Figure 3, which applies for the largest manifold flow tested, illustrates the variation in velocity profile with distance from the manifold. The vertical location of the maximum velocity is seen to rise with increasing x, so that at $x = 12$ in. ($x/D = 12/1.25 = 10$) the maximum velocity occurs at the surface; this behavior, for an initially submerged jet, has been documented by Mross (1960). For $x > 12$ in., the velocity profiles do become quite linear.

Figure 4 incorporates data in the "fully developed" region for three discharge rates; all data have been put in non-dimensional form and compared to the normal distribution equation,

$$\frac{v}{v_{max}} = e^{-y/2S^2} \qquad (1)$$

where S is defined as the depth y below the free surface at which the velocity is equal to 0.605 v_{max}, with v_{max} occurring at the free surface. Thus, the current is seen to have a typical turbulent jet mixing profile following the relationship (Eq. 1) used by Albertson et al (1950). It is seen also that the velocity profile could indeed be closely approximated by the linear velocity distribution incorporated in the theory of Taylor.

Figure 5 illustrates, again for three discharges, the growth of the nominal current thickness h with distance. The rate of growth of h with x in the fully developed region is 1:8, which is nearly the same as that measured by Williams for a manifold discharging at (not below) the free surface and containing relatively fewer and much larger discharge ports. The 1:8 spread ratio is also consistent with values for the vertical spread of single neutrally buoyant jets reported by Jen et al (1966).

Finally, Figure 6 indicates that horizontal momentum is indeed conserved in the surface current created by the jets discharging from the manifold, at least for x - distances within which the current's effect on the incident waves was observed. Again, results are compared with those of Williams. The value of the momentum flux per foot of width in the jets leaving the manifold was calculated by:

$$M_o = q\rho q \frac{1}{a_o} = \frac{q^2 \rho}{a_o} \qquad (2)$$

where for the experiments described $a_o = 4.05 \times 10^{-4}$ ft^2/ft, the total area of orifices per foot of width. Because the orifice diameter was only 0.04-in., compared to the 0.125-in. wall thickness, the orifices could be treated as tubes flowing full at exit. Values of the current momentum M_c at the various stations were obtained by integration of the velocity profiles.

Momentum Correlation of Attenuation Results - The foregoing results have been reviewed as justification and background for correlating the wave attenuation data on a momentum basis. Various manifold geometries could produce the same momentum flux magnitude at the same x - distance from the manifold; consequently, initial energy and power inputs to identical surface currents created by the hydraulic breakwaters could vary. Currents created by manifolds of different geometries have been seen to be comparable and well-behaved from a momentum standpoint. The momentum of the jets leaving the manifold usually may be estimated readily.

Accordingly, the initial jet momentum M_o has been selected as one of the independent parameters. (It might be noted that Taylor implies the wave stopping ability of a surface current to be dependent upon its "flow of inertia" - i.e., momentum flux).

Lamb (1932, Section 250) has shown that surface waves of finite amplitude possess momentum which is directed parallel to the direction of wave propogation. For deep water waves in still water the following expression is given:

$$\text{Mom/wave length/unit width} = \pi\rho a^2 c \tag{3}$$

where a is the wave amplitude and c is the celerity. If Eq. 3 is multiplied by (wave length/unit time) in order to express results in terms of average momentum/unit time/unit width, the result is

$$M_w = \pi\rho a^2 c \left(\frac{c}{L}\right) = \frac{\pi\rho a^2 c^2}{L}$$

For deep water waves, where $c = \sqrt{gL/2\pi}$ substitution gives

$$M_w = \frac{\rho g a^2}{2} = \frac{\rho g H^2}{8} \tag{4}$$

where a is assumed to be one-half the wave height, H.

It is noted in passing that M_w as given in Eq. 4 is equal to the total energy density computed from small-amplitude wave theory and is twice the "radiation stress" defined by Longuet-Higgins and Stewart (1964) as the excess flow of momentum due to the presence of small amplitude waves.

Without proceeding through a formal dimensional analysis, for a given manifold configuration (i.e., size, submergence, and initial direction of discharge) the wave attenuation can be expressed as

$$\eta = \eta\left(\frac{M_o}{M_w}, \frac{H}{L}, \frac{L}{d}\right) \tag{5}$$

where:

$\eta = \frac{H-H_t}{H}$, the wave attenuation

$\frac{H}{L}$ = wave steepness

$\frac{M_o}{M_w}$ = relative momenta of current and waves

$$= \frac{g^2 \rho}{\lambda^2 \omega^4}$$

$$\frac{\rho g H^2}{8}$$

For deep water waves it might be anticipated that

$$\eta = \eta\left(\frac{M_o}{M_w}, \frac{H}{L}\right) \tag{6}$$

only, as L/d should no longer be significant. This hypothesis must be examined in light of the test data.

Typical experimental data for one particular value of L/d (here, 0.375) are shown in Figure 7. These results show the effects of variation in manifold discharge (hence, current momentum) for different amplitude waves of the same wave length. Trends in the data are different at low discharges from those at higher flows. Finite attenuation occurs at zero discharge, due to the finite-sized circular manifold submerged just below the free surface. This result differs from the potential flow solution of Dean (1948), which predicted no difference in amplitude between incident and transmitted waves at great distances on either side of a submerged circular cylinder. As noted, the wave gage was not "far" from the manifold. However, at zero discharge the greatest attenuation took place for the shorter waves which in turn would have had a relatively longer distance in terms of wave length in which to reform after passing the manifold. At zero discharge and at the lower manifold discharges there is relatively greater attenuation for the larger (steeper) waves. When the manifold was discharging, distinct reduction in wave heights occurred upstream from the manifold, so for $q>0$ the entire attenuation is credited to the action of the surface currents. Phase shifts occurred as the waves reformed on the lee side of the manifold; as previously noted, the gage may have been too close to the manifold for the longer wave lengths so at the larger L/d values tested the experimental values of η could be somewhat large. For the higher discharges, greater attenuation is obtained with the waves of smaller amplitude; wave steepness no longer appears to be as significant as wave amplitude. For a particular L/d, as typified by the data of Figure 7, no consistent trend of attenuation with respect to wave steepness is apparent.

Results for all the wave attenuation tests are given in Figure 8, in which η is plotted against the relative momenta, M', defined as

$$M' = \frac{M_o}{M_w} = \frac{8q^2}{g\, a_o H^2} \tag{7}$$

Within reasonable limits and for significant non-zero values of M', η is dependent upon wave steepness but independent of L/d. The hypothesis of Eq. 6 is justified. For a given M', the steeper the wave the greater the degree of attenuation. Or, for complete "stopping" (i.e., $\eta = 1.0$), waves of decreasing steepness require relatively greater values of momentum in the surface current.

The overlapping results for small values of both M' and η can be attributed to experimental error and to the presence of the manifold cylinder. In light of the possible sources of experimental error, the greatest validity is attributed to the data showing the larger values of η. Further, these larger attenuation values are the ones of practical interest in possible applications of the hydraulic breakwater. For these significant values of η, which also can be attributed entirely to the surface current without consideration of the size of the manifold obstruction, the dependency of η upon H/L is shown further in Figure 9.

Figure 9 is a replot of the curves of Figure 8, with consideration limited to $\eta > 0.3$. The curve for $\eta = 1.0$ is shown as a dashed line to indicate that it is an approximation obtained by extrapolation of the curves of Figure 8 to $\eta = 1.0$; these extrapolations shown on Figure 8 are used and not the test values for which $\eta = 1.0$ because runs were made at particular discrete values of q and flows were not adjusted in an attempt to find the lowest manifold discharge which produced complete wave attenuation.

As H/L approaches the 0.142 value which is the theoretical steepness at which breaking occurs for deep water waves of finite amplitude, the values of M' do indeed decrease to small values for the 0.3-1.0 range of η shown. For decreasing wave steepnesses there is a monotonic increase in M' required for the same degree of attenuation. Also, for smaller H/L values, the range of M' required to achieve the 0.3-1.0 range of η is much greater than for the steeper waves.

Comparison with Prior Theory - The results of Taylor's theory for the complete stopping of waves by an opposing surface current of finite thickness and linearly varying velocity can be summarized in terms of the critical relationship between two parameters, α_2 and Z_2, defined as

$$\alpha_2 = \frac{gT}{2\pi v_{max}} = \frac{1}{v_{max}}\sqrt{\frac{gL}{2\pi}} = \frac{c}{v_{max}} \qquad (8)$$

for deep water waves

and $$Z_2 = \frac{gh}{v_{max}^2} . \qquad (9)$$

If α_{2m} is defined as the value of α_2 for the case where deep water waves are completely stopped by the opposing current, a plot of α_{2m} vs. Z_2 as prepared from Taylor's results divides the $\alpha_{2m} - Z_2$ plane into two regions, the region below the curve where waves are completely stopped by a surface current described by Z_2 and the region above the curve where the opposing current does not stop the waves. Figure 10 shows the results of the theory.

Some experimental data for the present study are shown on Figure 10; these data were obtained for runs during which complete wave attenuation ("stopping") occurred. Results are subjective, because the criterion used for selecting the station at which the critical stopping current was present was to select by visual observation that station closest to the breakwater beyond which a particular wave would not advance. Because both Z_2 and α_{2m} were evaluated from measured current velocities in still water at the $\bar{x}$- distance so selected, the test points plotted in Figure 10 must be looked on as subjective.

The limited test data do not match the theoretical prediction. In addition, the present deep water results deviate further from Taylor's theory than do the results of Williams which are shown also on Figure 10, and the smaller the value of L/d the greater the deviation from the theory. The inference to be drawn from the values shown on Figure 10 is that the maximum wave length that can be stopped by a given current is, based on experiment, considerably shorter than predicted by Taylor's theory. However, because the theory neglects the wave height (which has been shown to be significant and is incorporated in both M' and H/L) it must be considered as an initial guide only as it predicts performance which is considerably better than the experiments indicate to be possible with hydraulic breakwaters.

CONCLUSIONS, CONSIDERATION OF POSSIBLE FIELD APPLICATIONS

The significant quantitative findings of this study are shown in Figures 8 and 9. The wave attenuation performance of hydraulic breakwaters has been correlated on the basis of the relative momenta of the breakwater's surface current and of the incident waves. Previous investigators (Straub et al, Williams) have demonstrated that the Froude scaling law may be applied to experiments on hydraulic breakwaters. Further, the results of Figure 9 can be used in initial design calculations in which the feasibility of using hydraulic breakwaters under specified wave conditions can be considered. An illustration is given below.

The example selected is based on a particular prototype situation which suggested the study; physical characteristics of the site have been detailed by Richey (1968). A floating highway bridge spanning a lake was observed to cause undesirable reflected waves, and a hydraulic breakwater attached outboard of the bridge was considered briefly as one possible method of reducing the amplitude of the waves reflected from the structure. A typical wave encountered on the 200-foot deep lake has a length of 20 feet, corresponding to a wave period of approximately 2 seconds; a wave height which could be considered a significant wave is a value of H = 2 feet, although infrequent waves of greater height do occur at the location in question. The wave steepness is H/L = 2/20 = 0.10. Two degrees of attenuation ($\eta = 1.0$, $\eta = 0.5$) will be considered. Less than complete attenuation should be considered because the decay with travel upwind of the reflected waves may reduce them to more acceptable heights. The calculations tabulated below assume nozzles of the diameters specified spaced at 1-foot centers.

From Eq. 4, for the 2-foot wave, M_w = 31.2 lb/ft for the fresh water situation. Then, using the results of Figure 9:

$$\eta = 1.0,\ M' = 2.0,\ M_o = 62.5 \text{ lb/ft}$$
$$\eta = 0.5,\ M' = 0.8,\ M_o = 25.0 \text{ lb/ft}$$

Considering the nozzles to discharge full-sized streams with no contraction, the following figures result:

η	D_o - in	a_o - ft^2/ft	q - cfs/ft	v_o - fps	HP/ft
1.0	1	0.00545	0.42	77.0	4.38
	2	.0218	0.84	38.5	2.19
	3	.0492	1.26	25.6	1.46
	4	.0872	1.68	19.2	1.10
0.5	1	.00545	0.27	48.6	1.10
	2	.0218	0.53	24.3	0.55
	3	.0492	0.80	16.2	0.37
	4	.0872	1.06	12.1	0.27

The complete attenuation requirement for the specified wave leads to large power requirements, but the η = 0.5 case gives requirements which are more reasonable. In this regard it must be noted that losses in the piping system necessary to supply the breakwater manifold have not been included.

On the other hand, the "2-second" wave considered above is much shorter than the maximum wave lengths observed at the site in question. Waves of period T = 3 seconds are not uncommon and will be considered here, again for the 2-foot wave height H. For H/L = 2/46 = 0.0435, the following are obtained from Figure 9: if η = 1.0, M' = 9.5; if η = 0.5, M' = 5.5 Assuming 4-inch nozzles at 12-inch spacing (a_o = .0872 ft^2/ft) and a wave attenuation of η = 0.5, the following values result: q = 2.77 cfs/ft, v_o = 31.8 fps, jet power = 4.94 HP/ft. The power requirement is unrealistically high. Further, it may be noted that the M' = 0.8 value which provided η = 0.5 for the 2-second wave is virtually useless and insignificant for the 3-second wave.

It has been demonstrated that counter current producing breakwaters (if it may be assumed that essentially comparable results apply for the pneumatic as well as for the hydraulic devices) follow the general trend of other breakwaters, i.e., being most effective for shorter, steeper waves. Used as a breakwater in the conventional sense, the hydraulic breakwater appears too inefficient and costly for deep water as well as for shallow water waves. However, if reflected waves which lead to cross-wave patterns which in turn may be very undesirable and can be considered a form of water pollution, then as with other types of water pollution the costs inferred from the foregoing sample calculations might be acceptable if there is sufficient demand to eliminate the "pollution." One possibility would be the installation of hydraulic breakwaters around entrances to pontoon-type marinas for which fixed wave attenuators or energy absorbers might not be feasible and where elimination of reflected waves is desired in order to increase the safety and maneuverability of small boats operating in the near vicinity; in such a situation, intermittent operation of relatively short hydraulic breakwaters might be justified.

REFERENCES

Albertson, M. L., Dai, Y. B., Jensen, R. A. and Rouse, H., "Diffusion of Submerged Jets", Transactions ASCE, Vol. 115, 1950, pp. 639-664.

Dean, W. R., "On the Reflexion of Surface Waves by a Submerged Circular Cylinder", Proceedings of the Cambridge Philosophical Society, Vol. 44, 1948, pp. 483-491.

Evans, J. T., "Pneumatic and Similar Breakwaters", Proceedings of the Royal Society, A, Vol. 231, 1955, pp. 457-466.

Hsu, E. Y., "A Wind, Water-Wave Research Facility", Tech. Report No. 57, Department of Civil Engineering, Stanford University, Oct. 1965.

Jen, Y., Wiegel, R. L. and Mobarek, I., "Surface Discharge of Horizontal Warm-Water Jet", Proceedings ASCE, Vol. 92, No. PO 2, April, 1966, pp. 1-30.

Lamb, H., "Hydrodynamics", 6th Edition, Dover Publications, New York, 1945.

Longuet-Higgins, M. S. and Stewart, R. W., "Radiation Stresses in Water Waves: a Physical Discussion, with Applications", Deep-Sea Research, Vol. 11, 1964, pp. 529-562.

Mross, J. J., "The Effect of a Free Surface Upon the Velocity Distribution of a Submerged Jet", M. S. Thesis, State University of Iowa, 1960, (unpublished)

Richey, E. P., "Upwind Travel of Reflected Waves", Proceedings of the Eleventh Conference on Coastal Engineering.

Straub, L. G., Herbich, J. B., and Bowers, C. E., "An Experimental Study of Hydraulic Breakwaters", Proceedings of the Sixth Conference on Coastal Engineering, Council on Wave Research, 1958, pp. 715-728.

Taylor, G. I., "The Action of a Surface Current Used as a Breakwater", Proceedings of the Royal Society, A, Vol. 231, 1955, pp. 466-478.

Williams, J. A., "Verification of the Froude Modeling Law for Hydraulic Breakwaters", Tech. Report No. 104-11, Institute of Engineering Research, University of California, Berkeley, Aug. 1960.

Williams, J. A. and Wiegel, R. L., "Attenuation of Wind Waves by a Hydraulic Breakwater", Proceedings of the Eighth Conference on Coastal Engineering, Council on Wave Research, 1963, pp. 500-520.

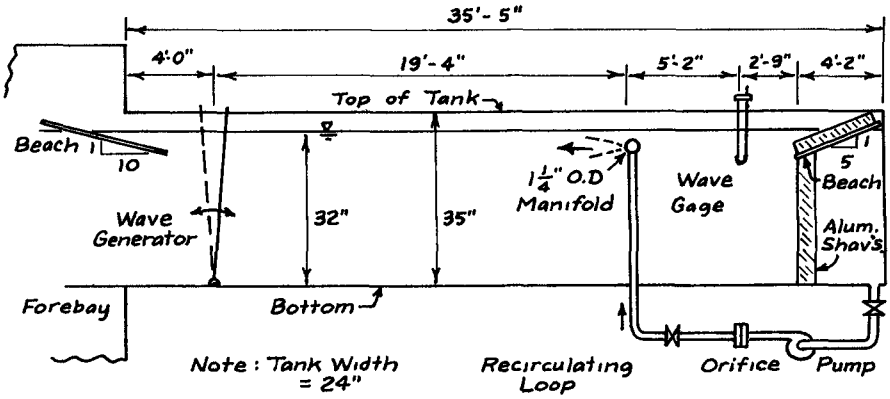

Fig. 1. Schematic Diagram of Laboratory Facility.

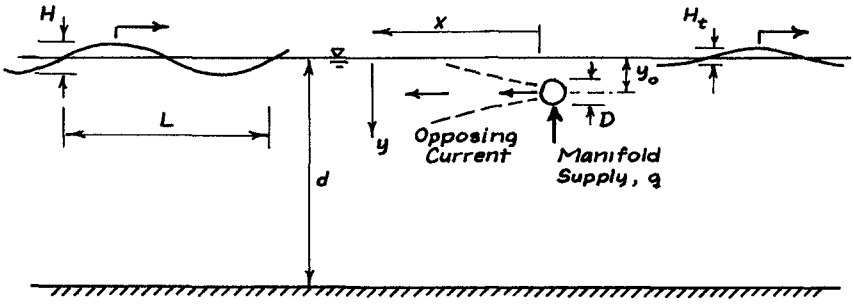

Fig. 2. Definition and Notation Sketch.

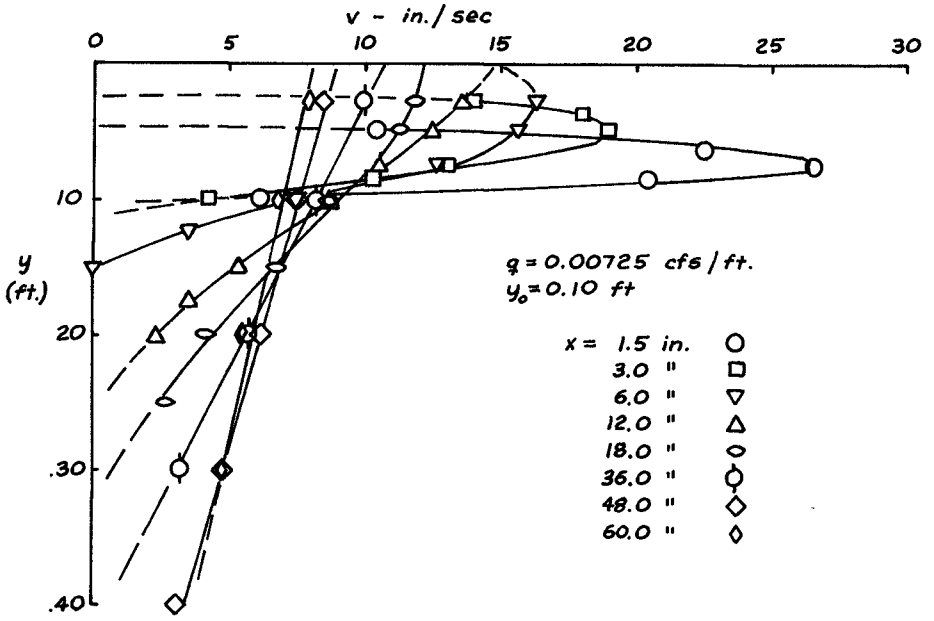

Fig. 3. Variation in Surface Current Velocity Profiles with Distance from Manifold.

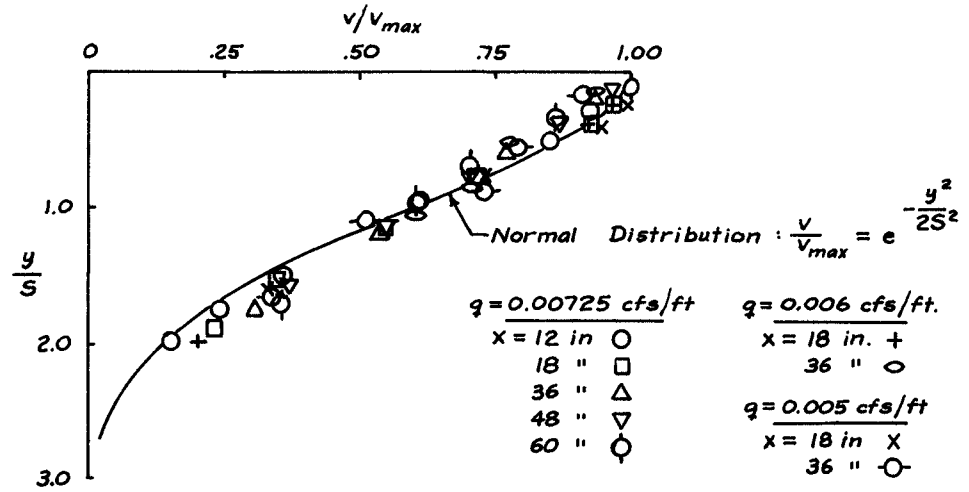

Fig. 4. Comparison of Velocity Profiles with Normal Distribution.

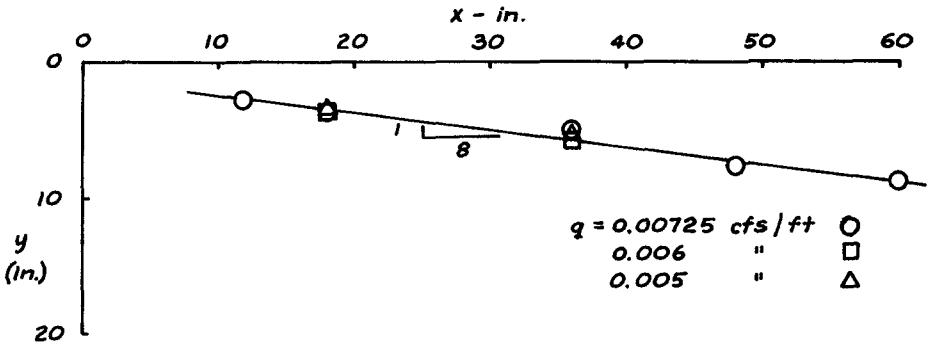

Fig. 5. Growth of Surface Current Thickness.

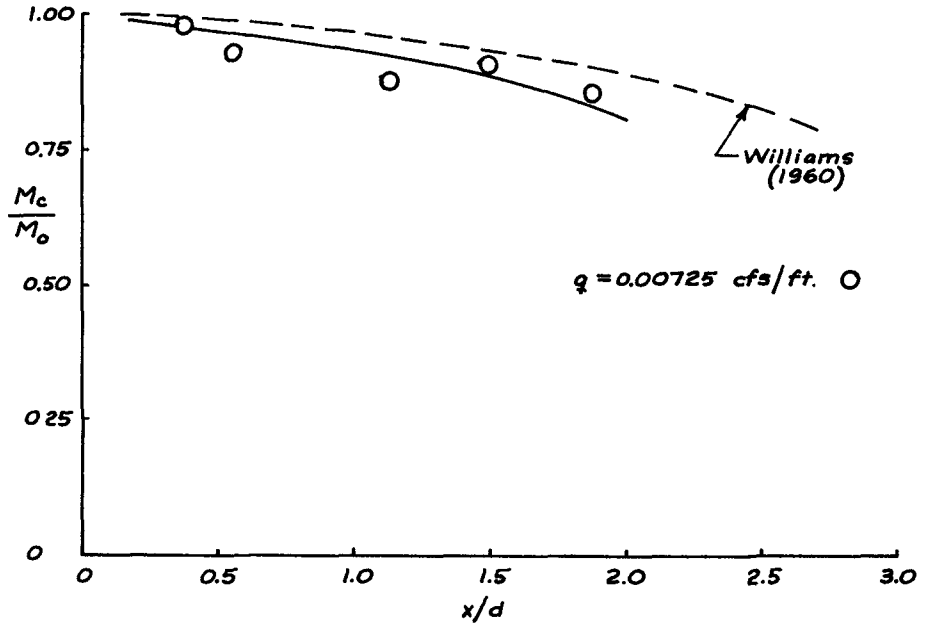

Fig. 6. Variation of Surface Current Momentum Flux with Distance from Manifold.

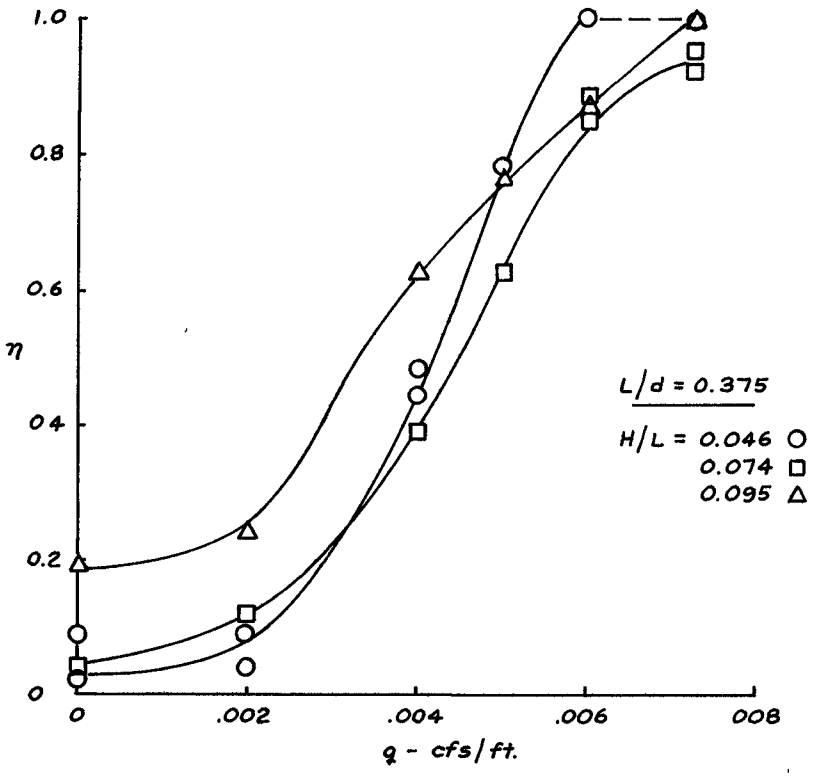

Fig. 7. Typical Wave Attenuation Data for L/d = Constant, H/L Varying.

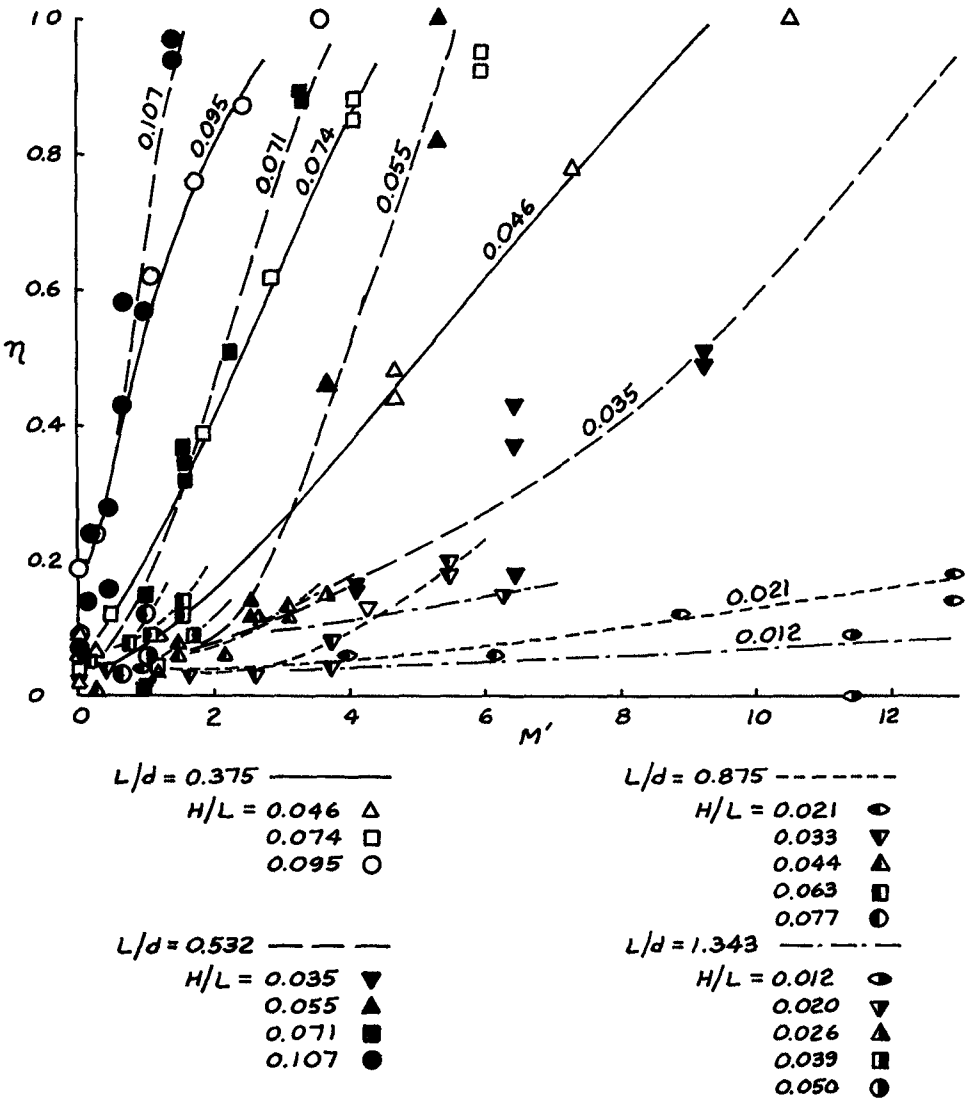

Fig. 8. Summary of Experimental Results, Wave Attenuation vs. Momentum Ratio.

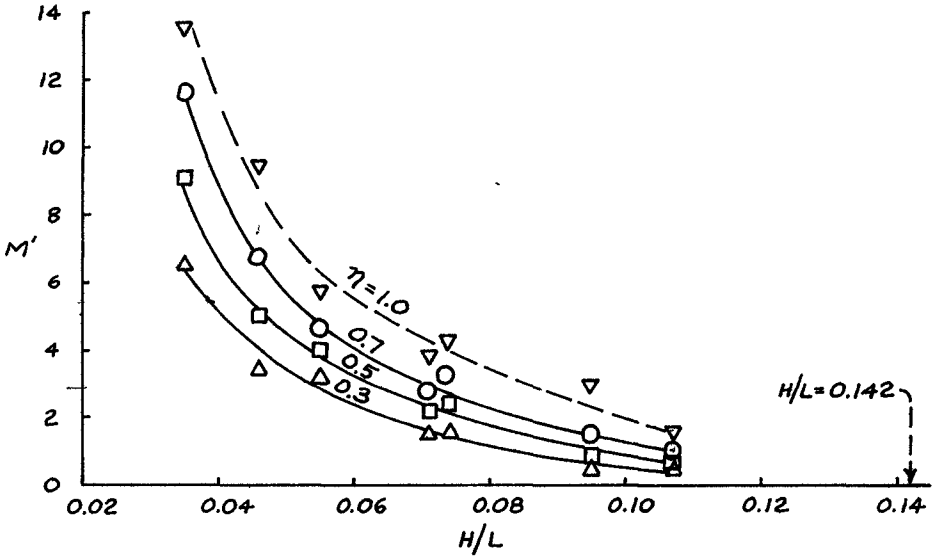

Fig. 9. Effect of Wave Steepness on Momentum Ratio Required for Specified Attenuation.

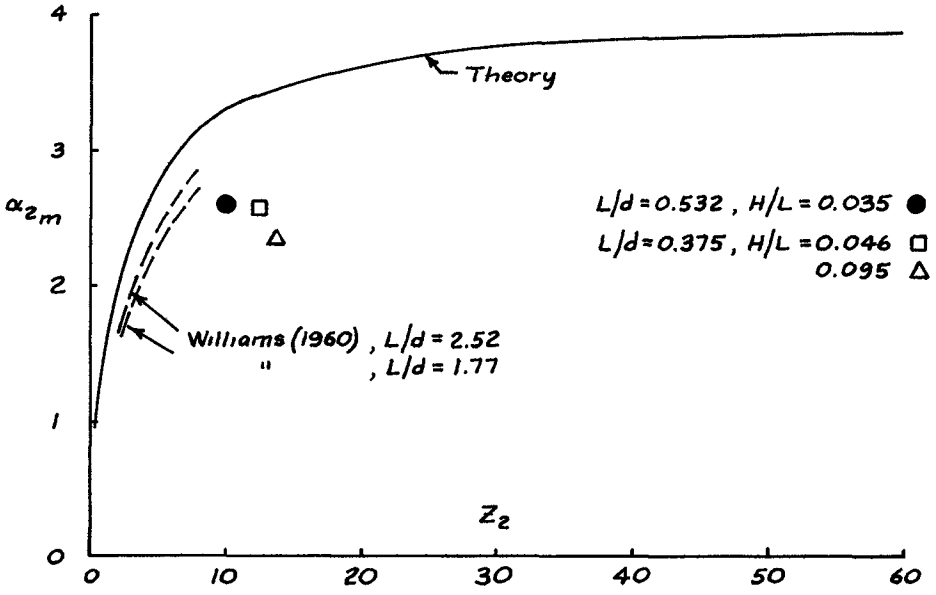

Fig. 10. Comparison with Theory of Taylor.